LUND UNIVERSITY

Impact of matching network on bandwidth of compact antenna arrays

Lau, Buon Kiong; Bach Andersen, Jørgen; Kristensson, Gerhard; Molisch, Andreas

Published in:
IEEE Transactions on Antennas and Propagation

DOI:
10.1109/TAP.2006.883984

2006

Document Version:
Peer reviewed version (aka post-print)

Link to publication

Citation for published version (APA):
Lau, B. K., Bach Andersen, J., Kristensson, G., & Molisch, A. (2006). Impact of matching network on bandwidth of compact antenna arrays. *IEEE Transactions on Antennas and Propagation*, *54*(11), 3225-3238. https://doi.org/10.1109/TAP.2006.883984

Total number of authors:
4

General rights
Unless other specific re-use rights are stated the following general rights apply:
Copyright and moral rights for the publications made accessible in the public portal are retained by the authors and/or other copyright owners and it is a condition of accessing publications that users recognise and abide by the legal requirements associated with these rights.
• Users may download and print one copy of any publication from the public portal for the purpose of private study or research.
• You may not further distribute the material or use it for any profit-making activity or commercial gain
• You may freely distribute the URL identifying the publication in the public portal

Read more about Creative commons licenses: https://creativecommons.org/licenses/

Take down policy
If you believe that this document breaches copyright please contact us providing details, and we will remove access to the work immediately and investigate your claim.

LUND UNIVERSITY

PO Box 117
221 00 Lund
+46 46-222 00 00

Download date: 17. Dec. 2025

Impact of Matching Network on Bandwidth of Compact Antenna Arrays

Buon Kiong Lau, *Member, IEEE*, Jørgen Bach Andersen, *Life Fellow, IEEE*, Gerhard Kristensson, *Senior Member*, *IEEE*, and Andreas F. Molisch, *Fellow, IEEE*

***Abstract*—We analyze the impact of the matching network on compact MIMO systems. Existing studies have found that the matching network has a significant influence on the performance of multiple antenna systems when the antennas are in close proximity. However, none has examined the wideband case. In this paper, we investigate the wideband performance of four different matching networks for multiple dipole antennas. The performance of the matching networks is given in terms of the bandwidths of correlation and matching efficiency, which are extensions of the single-antenna concept of bandwidth to multiple antenna systems. We also investigate the impact of the propagation conditions on the matching and bandwidth. For a uniform 2D angular power spectrum, we find that while individual-port matching can achieve in excess of 3% fractional correlation bandwidth for envelope correlation of 0.5 at an antenna separation of 0.01λ, multiport matching is required for efficiency bandwidth to exist for a return loss of −6dB. Moreover, even with multiport matching, both correlation and efficiency bandwidths decrease drastically at small antenna separations. At 0.01λ, the correlation and efficiency bandwidths are 0.4% and 0.2%, respectively. Similar evaluations were performed for measured outdoor-to-indoor channels with moderate to small 2D angular spreads. We find that the efficiency advantage of multiport matching over individual-port matching diminishes with decreasing angular spread.**

***Index Terms*— Antenna arrays, mutual coupling, impedance matching, correlation, antenna efficiency.**

I. Introduction

MIMO (multiple-input-multiple-output) systems make use of multiple antennas at both the transmitter and receiver ends to exploit the spatial channel for increasing the capacity [1]-[6]. The advantages of MIMO systems are well known, and have led to a large number of publications, as well as the emergence of commercial systems based on this technology.

Correlation of the signals at the different antenna elements can considerably decrease the capacity of a MIMO system [7]. Such correlation occurs particularly for compact MIMO systems, where the separation between the antennas is small; this effect has been investigated extensively [8]. In addition, for a small separation, the effect of mutual coupling between the antennas becomes important. It is well known that mutual coupling distorts antenna patterns and therefore modifies the correlation results [9], [10]. The change in input impedances of the antennas is another consequence of mutual coupling, and it results in greater mismatch between the antennas and their corresponding source and load impedances [11].

Many existing studies present interesting results on the impact of mutual coupling on the performance of narrowband compact multiple antenna systems in different propagation environments. While some describe correlation or diversity gain performance [9]-[15], others consider radiation efficiency [11], [16], and capacity [13]-[20]. In particular, conflicting views arise on the impact of mutual coupling on capacity performance, with some claiming mutual coupling effects to be beneficial for capacity [13], while others either completely disagree [14], [18], [19], or indicate that its benefits apply only to selected cases (e.g. a range of antenna separations) [15], [16]. The discrepancy is largely due to different assumptions on the system setup, e.g. whether the transmit power or source voltage is kept constant. Antenna matching has an important impact on these assumptions. However, with the exceptions of [12] and [16], these studies only employ simple matching circuits (such as 50Ω and open circuit terminations).

The use of S-parameter representation to model an entire narrowband communication system was proposed in [12], [16] and [20]. Using this approach, a more diverse range of matching networks, including optimum multiport matching, has been studied in the context of antenna correlation and diversity gain [12] and capacity [16]. The results indicate the importance of matching network in the performance of narrowband MIMO systems [12], [16].

While the narrowband studies in [12] and [16] give valuable insights into the performance of compact antenna systems, many newer wireless communications systems such as WCDMA and IEEE802.11a are wideband, in the sense that the antenna system of these wireless devices are required to operate within sizeable fractional bandwidths. While

Manuscript received September 15, 2005. This work was supported in part by the VINNOVA under grant no. P24843-3.

B. K. Lau is with the Department of Electroscience, Lund University, SE-221 00 Lund, Sweden (e-mail: bklau@ieee.org).

J. B. Andersen is with the Department of Communication Technology, Aalborg University, DK-9220 Aalborg, Denmark (e-mail: jba@kom.aau.dk).

G. Kristensson is with the Department of Electroscience, Lund University, SE-221 00 Lund, Sweden (e-mail: Gerhard.Kristensson@es.lth.se).

A. F. Molisch is with Mitsubishi Electric Research Laboratories, Cambridge, MA 02139 USA and also at the Department of Electroscience, Lund University, SE-221 00 Lund, Sweden (e-mail: Andreas.Molisch@ieee.org).

narrowband matching can be made ideal, wideband matching has fundamental theoretical as well as practical limits. Therefore, it is crucial to study the wideband performance of such antenna systems for successful implementations in future systems.

In this contribution, we extend the approach of [12] to study the impact of four different matching networks on the performance of wideband systems. They include the characteristic match, self impedance match, and multiport conjugate match [12], as well as a novel individual-port *input impedance match* [21], [22], which under uniform 3D angular power spectrum gives zero antenna correlation for any antenna separation. We show numerically how the wideband compact antenna systems perform with different matching networks according to the extent of their matching to the self and mutual impedances of the antennas.

As opposed to the single antenna case, where the bandwidth performance is uniquely defined with respect to a given return loss, there exists no standard definition of bandwidth for multiple antennas. This is because the performance of multiple antennas depends on their transmit (or radiation) and receive efficiencies, as well as the correlations among the received signals at the output of the antenna systems, the latter two of which also depend on the effects of the propagation environment. With this in mind, we define antenna correlation and matching efficiency for multiple antennas. We differentiate between transmit and receive matching efficiencies. The concept of bandwidth is then applied to each of these criteria. Correlation (or efficiency) bandwidth is then the frequency range in which the correlation (or efficiency) satisfies a given minimum performance threshold.

We begin this paper with an introduction to the system model in Section II. Four different matching conditions and their respective implementations are described in Sections III and IV. In Section V, we define the two performance measures used in our study: antenna correlation and matching efficiency, as well as the concept of bandwidth as derived from them. This is followed by numerical and simulation results in Sections VI, VII and VIII, which demonstrate the impact of matching networks on the performance of compact antenna systems in different propagation environments. In particular, we consider the classical uniform 2D angular power spectrum (APS) and the measured wideband outdoor-to-indoor channels [23]. For completeness and readers' convenience, we also incorporate reviews of the state of the art throughout the paper.

II. System Model

Figure 1 presents the simplified model of a $M \times N$ MIMO system. We assume downlink transmission, though the model is equally applicable for the uplink by reciprocity. The transmit and receive antenna arrays and the scatterers are assumed to be in the farfield of one another. For notational convenience, we do not explicitly show the frequency dependence of system parameters.

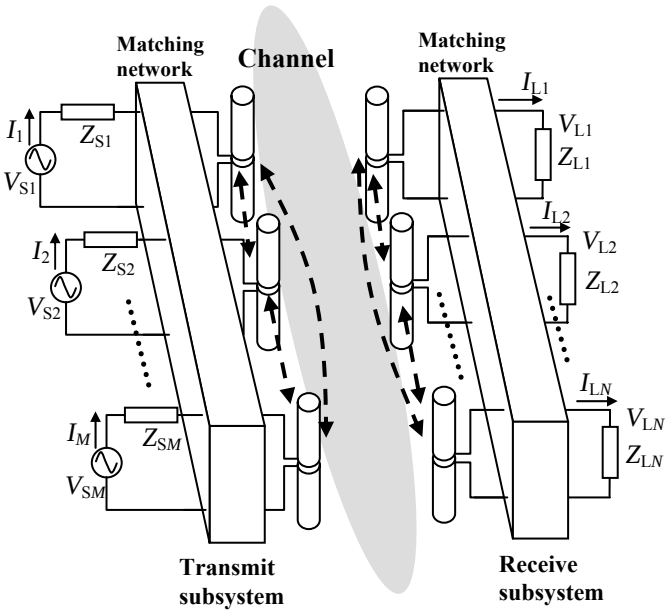

Fig. 1. A $M \times N$ MIMO communication system. Dashed line with arrowheads represent coupling between antennas.

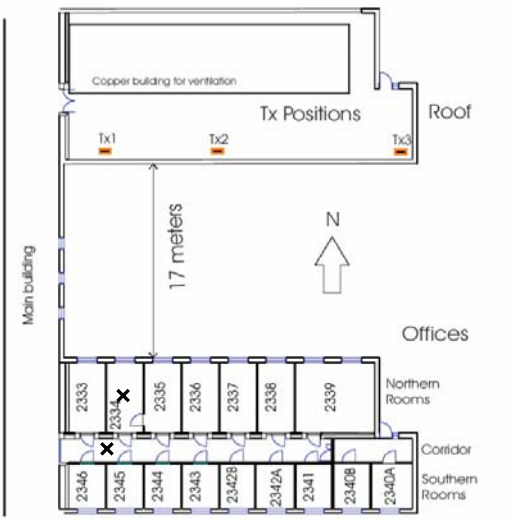

Fig. 2. Measurement site: three transmitter positions on the roof and 52 receiver positions in the offices 2334, 2336, 2337, 2339 ("Northern rooms"), 2345, 2343, 2342A, 2340B ("Southern rooms") and the corridor. LOS position (office 2334) and NLOS position (corridor) are indicated by crosses.

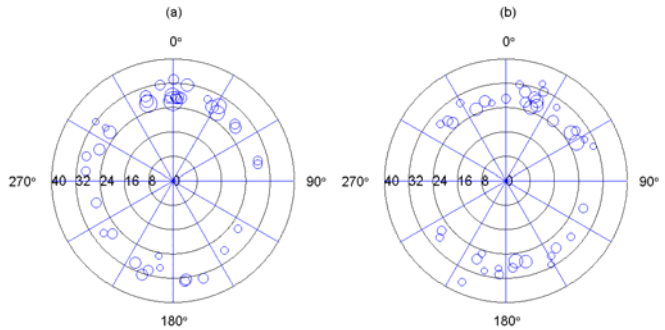

Fig. 3. DOA-delay plot in azimuth plane for (a) LOS and (b) NLOS positions. Larger circles indicate higher power of the MPCs. Radial axis in meters (with the delays expressed as the total distances traversed by the MPCs). North of the site map (see Fig. 2) and broadside of the dipole array correspond to 0°.

A. Transmit Subsystem

In the transmit subsystem or base station (BS), voltage sources V_{Si} with source impedance Z_{Si}'s are connected to a $M \times M$ matching network, which in turn feeds M antennas. The M-antenna configuration with separation distance d can be represented by a $M \times M$ impedance matrix $\mathbf{Z}_{TT}$. Due to its single-mode operation [24], the radiated field per unit feed current of the i-th antenna may be deduced from $\mathbf{Z}_{TT}$ and its azimuthal field $g_i^{T}(\theta)$ with all other antennas open-circuited. In our simulations, $g_i^{T}(\theta)$ is obtained using the method-of-moments (MoM) implementation of [25].

In our numerical evaluations, we analyze a 2×2 MIMO system. Vertically polarized half-wavelength ($\lambda/2$) electric dipole antennas of diameter $\lambda/400$ are approximated by thin strips of equal length and width of twice the diameter [25]. Although the dipole is uncommon in practice, its simplicity and well-studied behavior make it a popular reference case.

B. Propagation Channel

Both a frequency flat channel with uniform azimuthal APS and measured outdoor-to-indoor channels [23] are used for the numerical simulations; in both cases, 2D propagation is modeled, i.e., the elevation spread is neglected. The measured channels provide realistic channel responses in the angle and delay domains. Each realization of the propagation channel is characterized by its multipath components. Specifically, θ_l^{D}, θ_l^{A}, β_l, and τ_l are respectively the direction-of-departure (DOD), direction-of-arrival (DOA), complex gain and delay of the l-th multipath component (MPC).

The outdoor-to-indoor measurement campaign reported in [23] was performed with a RUSK ATM channel sounder at a center frequency of 5.2 GHz and a signal bandwidth of 120 MHz. The measurement environment is the "E-building" at LTH, Lund University, Sweden, an office building with brick walls and metal-coated windows. In total, 159 measurements were made for 3 transmit positions (Tx1-3) shown in Fig. 2 and 53 receive positions in the offices and corridor. For each transmit-receive position pair, the SAGE algorithm was used to extract 40 MPCs from 13 MIMO snapshots.

For the purpose of calculating correlation, we require a large number of realizations of the channel that has the same statistical properties. Due to shadow fading and different channel as seen by the transmit and receive positions, different measurement positions cannot be used for this purpose. Therefore, we employ the "random phase method" to synthetically generate 1000 channel realizations from the MPC data for a given transmit-receive position [26]. We note that as discussed in [26], the method is reliable especially for small number of array elements and when the MPC data (as extracted by SAGE) captures most of the receive power at the receive array. With this in mind, we selected two representative receive positions (for Tx1) with greater than 85% captured power for our study: (1) a "line of sight (LOS)" position with receiver in room 2334, RMS angular spread of 30°, RMS delay spread of 5.2 ns, and 95.8% captured power at a SNR of 19.2 dB, and (2) a "non-LOS (NLOS)" position with receiver in corridor, RMS angular spread of 51.8°, RMS delay spread of 5.1 ns, and 85% captured power at a SNR of 4.3 dB. These positions are indicated by crosses in Fig. 2 and the extracted MPCs are illustrated in Fig. 3(a) and 3(b). We note that our LOS designation is not strict, in that the "LOS position" does not only contain one dominant LOS path, but it also has several other dominant paths clustering around it (see Fig. 3(a)), which is in part due to reflections off the metal coated window. Moreover, the LOS path is itself attenuated by the double-pane window. Similarly, even though the "NLOS position" has no dominant path/cluster, the MPCs are largely confined to some azimuthal angular regions, thus giving it a moderate angular spread value.

C. Receive Subsystem

The receive subsystem or mobile station (MS) consists of N receive antennas, a $N \times N$ matching network, and N load impedance Z_{Lj}. As with the BS, the induced current per incident field of the jth antenna can be deduced from the impedance matrix of the receive antennas $\mathbf{Z}_{RR}$ and induced voltage for the open-circuit case $g_j^{R}(\theta)$, both of which are obtained from [25].

D. S-parameter Representation

Although the Z-parameter representation is often used to represent the communication blocks in Fig. 1, e.g. [10], it is convenient to use the S-parameter representation for investigating antenna correlation and matching efficiency. The Z- and S-parameter matrices are related by the transform $\mathbf{S} = \mathcal{F}(\mathbf{Z}) = (\mathbf{Z} + Z_0\mathbf{I})^{-1}(\mathbf{Z} - Z_0\mathbf{I})$, where Z_0 is the (real-valued) characteristic (or reference) impedance.

The block diagrams for the transmit and receive subsystems are given in Figs. 4 and 5, respectively. The matching network for both the transmit and receive subsystems is represented by the matrix [12]

$$\mathbf{S}_M = \begin{bmatrix} \mathbf{S}_{11} & \mathbf{S}_{12} \\ \mathbf{S}_{21} & \mathbf{S}_{22} \end{bmatrix}, \tag{1}$$

where "Side 1" (connected to the antenna ports) and "Side 2" (connected to the source or load) are indicated.

In Fig. 4, $\mathbf{S}_S$ and $\mathbf{S}_{TT} = \mathcal{F}(\mathbf{Z}_{TT})$ are the scattering matrices for the source impedances and transmit antennas, respectively. It is clear from Fig. 1 that $\mathbf{S}_S$ is diagonal. The input reflection coefficients of the matching network $\mathbf{\Gamma}_{in}$ is given by [12]

$$\mathbf{\Gamma}_{in} = \mathbf{S}_{22} + \mathbf{S}_{21}(\mathbf{I} - \mathbf{S}_{TT}\mathbf{S}_{11})^{-1}\mathbf{S}_{TT}\mathbf{S}_{12}. \tag{2}$$

In Fig. 5, the voltage sources represent the induced open-circuit voltages resulting from electromagnetic waves impinging on the receive antennas in the propagation channel. $\mathbf{S}_{RR} = \mathcal{F}(\mathbf{Z}_{RR})$ and the diagonal matrix $\mathbf{S}_L$ are the scattering matrices for the receive antennas and loads, respectively. We use the same notation $\mathbf{S}_M$ for the matching network, since for the purpose of this paper, we assume identical transmit and receive arrays, i.e., $\mathbf{S}_{TT} = \mathbf{S}_{RR}$. In this case, the input reflection coefficients of the matching network is given by

$$\mathbf{\Gamma}'_{in} = \mathbf{S}_{11} + \mathbf{S}_{12}(\mathbf{I} - \mathbf{S}_L\mathbf{S}_{22})^{-1}\mathbf{S}_L\mathbf{S}_{21}. \tag{3}$$

The voltage across the load network is given by [12]

$$\mathbf{v}_{\mathrm{L}} = Z_0^{1/2}\left(\mathbf{I}+\mathbf{S}_{\mathrm{L}}\right)\left(\mathbf{I}-\mathbf{S}_{22}\mathbf{S}_{\mathrm{L}}\right)^{-1}\mathbf{S}_{21}\left(\mathbf{I}-\mathbf{S}_{\mathrm{RR}}\boldsymbol{\Gamma}_{\mathrm{in}}^{'}\right)^{-1}\mathbf{b}_{\mathrm{R}}, \quad (4)$$

where the sources $\mathbf{b}_{\mathrm{R}}$ represent the excitation of the receive antennas from the impinging vertically polarized propagation waves E_0

$$\mathbf{b}_{\mathrm{R}} = c_1 E_0\left(\mathbf{I}-\mathbf{S}_{\mathrm{RR}}\right)\mathbf{g}_{\mathrm{T}}^{T}(\theta), \quad (5)$$

c_1 is a complex constant, $(\bullet)^T$ denotes transpose and the transmit radiation pattern $\mathbf{g}_{\mathrm{T}}(\theta) = \left[g_1^{\mathrm{T}}(\theta),\ldots,g_N^{\mathrm{T}}(\theta)\right]^T$ applies to the receive mode by reciprocity [12].

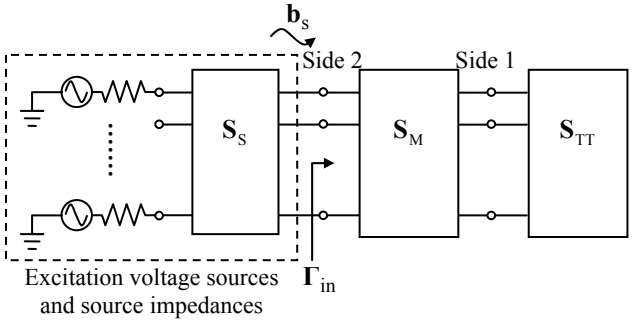

Fig. 4. Block diagram of transmit subsystem, with excitation voltage sources connected to a multiport matching circuit and antenna array.

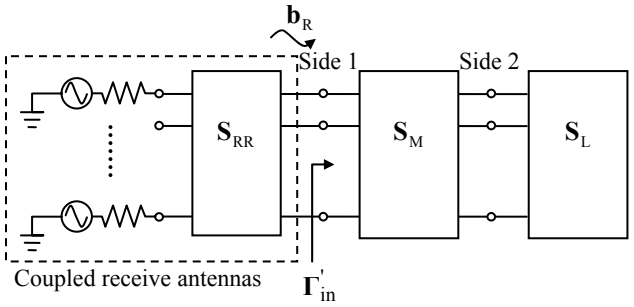

Fig. 5. Block diagram of the receive subsystem, with coupled antenna array connected to a multiport matching circuit and individual loads. The excitation voltages are given by the voltage across open-circuited antenna ports.

III. Matching Conditions

In this paper, we consider only lossless matching networks, so that $\mathbf{S}_{\mathrm{M}}^{H}\mathbf{S}_{\mathrm{M}} = \mathbf{I}$, where $(\bullet)^H$ denotes conjugate-transpose. Thus, only $\mathbf{S}_{11}$ and $\mathbf{S}_{22}$ need to be specified, while $\mathbf{S}_{12}$ and $\mathbf{S}_{21}$ can be obtained from

$$\mathbf{S}_{11}^{H}\mathbf{S}_{11} + \mathbf{S}_{21}^{H}\mathbf{S}_{21} = \mathbf{I}, \quad (6)$$

and

$$\mathbf{S}_{12}^{H}\mathbf{S}_{12} + \mathbf{S}_{22}^{H}\mathbf{S}_{22} = \mathbf{I}, \quad (7)$$

using singular value decomposition, as in [12]. There are infinitely many solutions of $\mathbf{S}_{21}$ and $\mathbf{S}_{12}$ that satisfy (6) and (7) [12]. In this paper, we obtain $\mathbf{S}_{21}$ and $\mathbf{S}_{12}$ using Cholesky factorization, which is uniquely defined for positive definite Hermitian matrix. Although by definition, a lossless matching network only guarantees positive semidefiniteness, practical matching networks such as those described in this paper ensures positive definiteness. Without loss of generality, we assume that

$$Z_{\mathrm{S}i} = Z_{\mathrm{L}j} = Z_0 = 50\Omega,\ i = 1,\ldots,M,\ j = 1,\ldots,N\ . \quad (8)$$

In the following, we introduce four different matching conditions, in the order of increasing goodness of the matching. Although the matching conditions are explained in the context of the receive mode in Fig. 5, they are equally applicable to the transmit mode in Fig. 4.

A. Characteristic Impedance Match

This is when the antennas are terminated with the load Z_0. In other words, there is no matching network. This can be modeled either by the removal of the matching network in Fig. 5, or by setting $\mathbf{S}_{11} = \mathbf{S}_{22} = \mathbf{0}$ and $\mathbf{S}_{21} = \mathbf{S}_{12} = \mathbf{I}$. The degree of mismatch depends on the difference between the antenna impedances and the characteristic impedance.

B. Self Impedance Match

As opposed to [12], where $\mathbf{S}_{11} = \mathrm{diag}\left(\mathbf{S}_{\mathrm{RR}}\right)^*$, where $\mathrm{diag}(\bullet)$ retains only the diagonal elements of the matrix operand, here we use the more common definition of the self impedance match, as given by

$$\mathbf{S}_{11} = \mathcal{F}\left[\mathrm{diag}\left(\mathbf{Z}_{\mathrm{RR}}^{*}\right)\right]. \quad (9)$$

For an isolated antenna, the self impedance match is also known as the complex conjugate match. It facilitates maximum power transfer to the load when there is no mutual coupling, i.e., the array antennas are infinitely far apart. At finite antenna separations, however, the goodness of the match depends on the behavior of the mutual impedance which is not taken into account. In this work, we also account for the slight variation in the self impedance (see Fig. 4 of [16]) due to the non-zero induced current along the length of the antenna in open-circuit condition.

C. Input Impedance Match

While the self impedance match only takes into account the self impedance of the antenna, the input impedance match also takes into account mutual coupling. The input impedance match attempts to conjugate-match the antenna pair individually (one at a time), i.e., there is a separate matching network for each port, and the Z-matrix of the matching network is diagonal. For the case of individual-port matching and where (8) is satisfied, the effect of the matching network of Fig. 1 can be represented by equivalent matching impedances Z_{M}. For a two-element transmit array, with one element (denoted "1") excited and the other (denoted "2") loaded with Z_{M}, the input impedance looking into the input ports of the excited antenna element (see Fig. 14) is given by

$$Z_{\mathrm{in}} = Z_{11} - Z_{12}^2 \big/ \left(Z_{22} + Z_{\mathrm{M}}\right), \quad (10)$$

where the mutual impedance $Z_{12} = Z_{21}$ by reciprocity and Z_{11} and Z_{22} are the self impedances of two antennas. Given that conjugate match requires $Z_{\mathrm{M}} = Z_{\mathrm{in}}^{*}$ (or equivalently, $\Gamma_{\mathrm{M}} = \Gamma_{\mathrm{in}}^{*}$ in S-parameters), we can solve for the "optimum" matching load either algebraically or iteratively. For the simple case of symmetrical dipoles ($Z_{11} = Z_{22}$), the unique solution as derived in the Appendix is given by

$$Z_{\mathrm{M}}^{\mathrm{opt}} = \sqrt{R_{11}^2 - R_{12}^2 + X_{12}^2 - \frac{R_{12}^2 X_{12}^2}{R_{11}^2}} + j\left(\frac{R_{12}X_{12}}{R_{11}} - X_{11}\right), \quad (11)$$

where $Z_{11} = R_{11} + jX_{11}$, $Z_{12} = R_{12} + jX_{12}$. We remark that the same expression applies to the receiving case, where the voltage source is now the induced (or open-circuit) voltage across antenna port 1.

Note that the "optimality" of the input impedance match refers to maximum power transfer from the single excited voltage source into the corresponding antenna port, which gives no consideration to power coupled into adjacent antenna(s). In fact, it has been found that the input impedance match *does not* correspond to the maximum radiated or received power for individual-port matching [28]. Instead, it facilitates low antenna correlation for any antenna separation. In the special case of a uniform 3D APS of the radiation, it gives zero antenna correlation! Further details are given in Section VI-A.

D. Multiport Conjugate (MC) Match

Like the input impedance match, the so-called multiport conjugate [16] (or optimal Hermitian [12]) match also takes account of the mutual coupling among the antenna ports. However, unlike the input impedance match, it allows the interconnections between all ports on the two sides of the network. The MC match requires one side of the matching network to be *conjugate-matched* to the antennas and the other side to the load, i.e. $\mathbf{S}_{11} = \mathbf{S}_{\mathrm{RR}}^H$ and $\mathbf{S}_{22} = \mathbf{S}_{\mathrm{L}}^H$. In our case of Z_0 termination, $\mathbf{S}_{22} = \mathbf{0}$.

IV. Matching Network Implementation

The self impedance match and input impedance match share the same basic property of being an individual-port match. This means that their corresponding "network" has no interconnecting ports on each side and thus $\mathbf{S}_{11}$ and $\mathbf{S}_{22}$ are diagonal. Individual-port match is well studied and many different implementations are possible for a given matching impedance value at the center frequency. In our study, we use the transmission line-open circuited stub configuration [27].

Though the condition for optimum matching of multiple antennas (or MC match) is well known [10], [12], [16], its practical implementation is a subject of current interest [29], [30]. Here, we implement the optimum matching proposed in [30], which is based on the more commonly used distributed elements (couplers, transmission lines and open-circuited stubs), as opposed to that of [29], which uses lumped elements. We also note that the authors of [30] appear to be unaware of [12], since the two papers appeared at around the same time. In fact, rather than optimum matching, the matching network in [30] was presented in the context of joint optimization for minimum envelope correlation and maximum matching efficiency. Moreover, due to the multimodal nature of the optimization problem, the $\mathbf{S}_{11} = \mathbf{S}_{\mathrm{RR}}^H$ condition for MC match at center frequency can only be approximated using the procedure in [30]. The goodness of the approximation varies according to the local solutions.

V. Performance Measures

A. Antenna Correlation

The calculation of (complex) antenna correlation ρ with S-parameters for different types of termination (or matching) is described in detail in [12]. The same expressions apply to our paper, apart from having frequency in addition to antenna separation as a parameter of interest.

B. Matching Efficiency

For a single antenna in transmit mode, the return loss resulting from mismatch between the source impedance Z_{S} and the antenna impedance Z_{A} is $\Gamma = (Z_{\mathrm{A}} - Z_{\mathrm{S}})/(Z_{\mathrm{A}} + Z_{\mathrm{S}})$. The proportion of power supplied to the antenna, or the matching efficiency, is defined by $\eta = 1 - |\Gamma|^2$. If the optimum matching network (self impedance match) is applied, then $\Gamma = 0$ and $\eta = 1$. In the receive mode, since the quantity of interest is the received load power, the efficiency may be measured with respect to the received load power, which by reciprocity is maximum with the self impedance match.

In the case of multiple antennas, the concept of matching efficiency becomes more complicated. For the transmit mode shown in Fig. 4, the inward and outward waves ($\mathbf{a}_{\mathrm{T}}$ and $\mathbf{b}_{\mathrm{T}}$) are related by the input scattering matrix (2)

$$\mathbf{b}_{\mathrm{T}} = \mathbf{\Gamma}_{\mathrm{in}}\mathbf{a}_{\mathrm{T}}. \quad (12)$$

Discounting ohmic losses in the antennas, the instantaneous radiated power is thus [16]

$$P_{\mathrm{inst}} = \mathbf{a}_{\mathrm{T}}^H\mathbf{a}_{\mathrm{T}} - \mathbf{b}_{\mathrm{T}}^H\mathbf{b}_{\mathrm{T}} = \mathbf{a}_{\mathrm{T}}^H\left(\mathbf{I} - \mathbf{\Gamma}_{\mathrm{in}}^H\mathbf{\Gamma}_{\mathrm{in}}\right)\mathbf{a}_{\mathrm{T}}. \quad (13)$$

For zero mean signals, the average radiated power is [16]

$$P_{\mathrm{T}} = \mathrm{E}\{P_{\mathrm{inst}}\} = \mathrm{tr}\left\{\mathbf{R}_{\mathbf{a}_{\mathrm{T}}}\left(\mathbf{I} - \mathbf{\Gamma}_{\mathrm{in}}^H\mathbf{\Gamma}_{\mathrm{in}}\right)\right\}, \quad (14)$$

where $\mathbf{R}_{\mathbf{a}_{\mathrm{T}}} = \mathrm{E}\left\{\mathbf{a}_{\mathrm{T}}\mathbf{a}_{\mathrm{T}}^H\right\}$. Based on (14), we introduce a new definition of transmit matching efficiency for the multiple antenna system as

$$\eta_{\mathrm{T}} = \mathrm{tr}\left\{\mathbf{R}_{\mathbf{a}_{\mathrm{T}}}\left(\mathbf{I} - \mathbf{\Gamma}_{\mathrm{in}}^H\mathbf{\Gamma}_{\mathrm{in}}\right)\right\} \Big/ \mathrm{tr}\left\{\mathbf{R}_{\mathbf{a}_{\mathrm{T}}}\right\}, \quad (15)$$

which is the ratio of average power radiated over the power supplied by the voltage sources into the matching network-antenna configuration. And since this network configuration consists of only passive elements $\eta_{\mathrm{T}} \le 1$. Moreover, since the antennas radiate finite power (or is lossy) by definition, and that cascade connection of lossless matching network to lossy antenna gives a lossy network, $\eta_{\mathrm{T}} > 0$.

For a transmit array of two identical antennas, and where the average signal power at the two ports are identical, (15) can be simplified to

$$\begin{aligned}\eta_{\mathrm{T}} = {} & \left(1 - |r_{11}|^2 - |r_{12}|^2\right) \\ & - 4\,\mathrm{Re}\left(r_{11}^* r_{12}\right)\mathrm{Re}\left(\mathrm{E}\left\{a_{\mathrm{T1}}a_{\mathrm{T2}}^*\right\}\right) \Big/ \mathrm{tr}\left\{\mathbf{R}_{\mathbf{a}_{\mathrm{T}}}\right\}.\end{aligned} \quad (16)$$

Furthermore, the last term in (16) disappears under the condition that the signals are uncorrelated, or when $r_{11} = 0$ or

$r_{12} = 0$ or $\mathrm{Re}\left(r_{11}^{*} r_{12}\right) = 0$.

Unlike the transmit mode, where full control over the input signals is possible, the extent to which the received signals at each port is related depends on the array pattern and spatial correlation. We define the receive matching efficiency η_{R} in the same manner as the *relative collected power* in [16], which is the ratio of the total received load power for the multiple antenna system to that of an optimally matched reference single antenna in the same environment. However, to ensure that the efficiency in the limiting case of infinitely separated antennas is equal to 1, we multiply the reference total power by the number of antennas. As in the transmit case, receive matching efficiency is bounded below by $\eta_{\mathrm{R}} > 0$, due to finite absorption of the receive antennas. However, unlike the transmit case, the receive efficiency is not bounded above by 1, since multiple receive antennas can be more efficient than a single receive antennas (see [16]).

C. Bandwidth

1) Efficiency Bandwidth

There is no single definition of the bandwidth of a single antenna. The term bandwidth simply represents a frequency range whereby the antenna operates within specifications. In wireless communications, it is commonly defined by the frequency range over which the return loss is less than a threshold level, e.g. $\gamma = -6$ dB (or 75% efficiency). The −6 dB threshold is a rule of thumb for the design of mobile terminal antennas.

As with matching efficiency, the bandwidth of a multiple antenna system differs from that of a single-antenna when mutual coupling effect becomes significant. To our knowledge, no standard definition has been proposed for bandwidth. This effort is further complicated by the influence of signal correlation over the radiated or received power, as explained in the previous section.

Nevertheless, if we focus solely on the property of the antenna, then it seems plausible to define the bandwidth of a multiple antenna system using the input coefficients $r_{ij} = \left[\boldsymbol{\Gamma}_{\mathrm{in}}\right]_{ij}$ from (2). The bandwidth is then the frequency range in which both its self-reflections r_{ii}'s and mutual reflections r_{ij}'s ($i \neq j$) satisfies a specified maximum return loss γ, i.e.,

$$\mathrm{BW} = 2\min\left[\min_{\forall i,j}\left(f_{ii}^{\mathrm{U}}, f_{ij}^{\mathrm{U}}\right) - f_c, f_c - \max_{\forall i,j}\left(f_{ii}^{\mathrm{L}}, f_{ij}^{\mathrm{L}}\right)\right], \quad (17)$$

where f_{ij}^{U} (and f_{ij}^{L}) are the first frequency higher (and lower) than the center frequency f_c at which $\left|r_{ij}\right|$ coincides with the specified return loss γ, given an initial level that is below γ at f_c. Where this condition is not met by all f_{ij}^{U}'s and f_{ij}^{L}'s, except when $\left|r_{ij}\right|$ is strictly less than γ, the bandwidth is then "undefined". In words, this implies that the bandwidth is specified by the dominant antenna reflection. The outermost "min" operator ensures that the bandwidth is symmetrical around the center frequency. This is a straightforward extension of the single antenna case which is commonly defined by its return loss. We shall henceforth refer to the bandwidth (17) as the efficiency bandwidth, since it is the range of frequency in which the matching efficiency is acceptable. We will illustrate and discuss the impact of matching network on efficiency bandwidth using plots of $\left|r_{11}\right|$ and $\left|r_{12}\right|$ in Section VIII.

A more comprehensive definition of bandwidth for multiple antenna system can be based on its matching efficiency in the transmit and receive modes. In the transmit mode with two identical antennas and average signal powers, if we assume that the input signals $\mathbf{a}_{\mathrm{T}}$ are uncorrelated, i.e., the last term of (16) drops out, then for a given total efficiency value (which corresponds to a total return loss) the resulting bandwidth based on (16) is closely approximated by (17), since it is dominated by the largest $\left|r_{ij}\right|$ at each of the lower and upper frequency edges.

In the receive mode, η_{R} has a strong dependence on the propagation condition, therefore one will need to take into account the typical operating environment in designing the antenna system. The receive efficiency bandwidth is then defined by the frequency in which η_{R} is above a specified efficiency level, i.e., $1 - \gamma^2$.

2) Correlation Bandwidth

Likewise, we can also consider the concept of bandwidth for antenna correlation. This is because antenna correlation plays an important role in the performance of MIMO and diversity antenna systems, and it is important that the correlation is kept under a threshold value for system gains to be realized. It is commonly accepted that the maximum envelope correlation ρ_e for good diversity gain is 0.5 [10], which corresponds to $\left|\rho\right| \approx 0.71$, since $\rho_e \approx \left|\rho\right|^2$. The correlation bandwidth can then be defined by the function $\left|\rho\right|$ in a manner similar to (17) for the threshold value $\left|\rho\right| = 0.71$.

VI. Numerical Results: Correlation

In this and the following two sections, we present simulation results for the impact of the different matching circuits on the wideband performance measures of antenna arrays. All the simulations assume that the transmit and receive arrays are sufficiently far apart that the far field assumption is valid, so that the channel models of Section II-B can be applied. Therefore, the simulations combine the plane-wave approximations for incident (or outgoing) fields with the MoM simulation of the fields on the antenna arrays [25]. The matching networks were implemented as discussed in Section IV.

It should be clear that induced (or open-circuit) voltages at the receive antennas are correlated, especially at small antenna separations. For any given induced voltage correlation, it is possible to find (for the receiving case) the optimum matching conditions for maximum power transfer [28]. Alternatively, one can optimize the matching condition for low antenna correlation [28]. We will show below that for a specific angular distribution, namely a uniform 3D APS, the antenna correlation with input impedance match or MC match is zero. However, this holds only at a specific frequency, and also one specific APS. This paper limits its scope to matching that does not take into account the propagation environment.

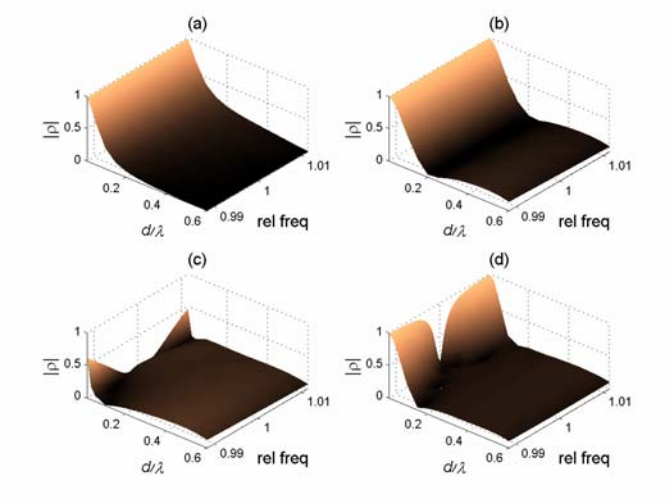

Fig. 6. Antenna correlation of uniform 2D APS at different antenna separations for different termination conditions: (a) Z_0 match, (b) Self impedance match, (c) Input impedance match, and (d) MC match.

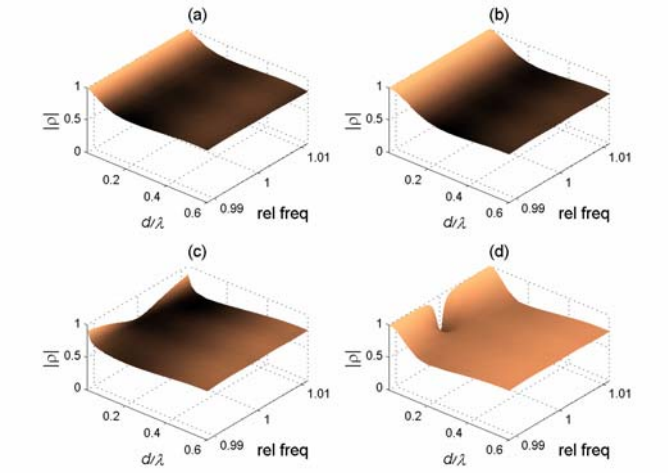

Fig. 7. Antenna correlation of LOS condition at different antenna separations for different matching: (a) Z_0 match, (b) Self impedance match, (c) Input impedance match, and (d) MC match.

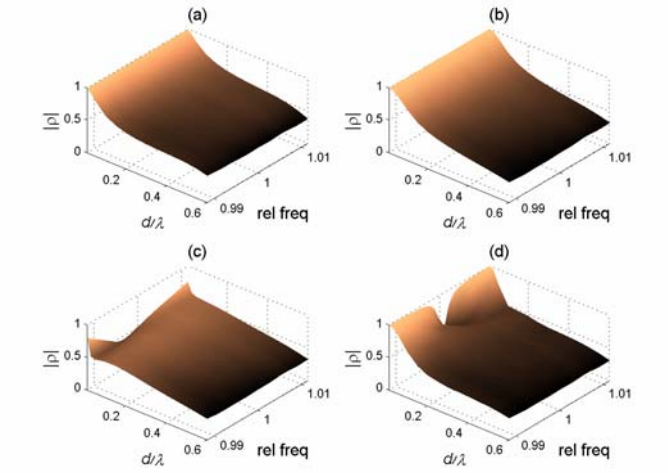

Fig. 8. Antenna correlation of NLOS condition at different antenna separations for different matching: (a) Z_0 match, (b) Self impedance match, (c) Input impedance match, and (d) MC match.

A. *Uniform 3D APS*

We first investigate a particular phenomenon, namely that at the center frequency, the input impedance match gives zero correlation for 3D uniform distribution of the radiation (see Section III-C). For the case of two identical antennas, this phenomenon can be explained analytically as follows: The input impedance match implies maximum power transfer (at the designed antenna separation and frequency) from the source into the load, which consists of the coupled antennas plus the adjacent circuits (see Fig. 14). This is equivalent to reflectionless matching from the perspective of the single excitation source and source load. Using the fact that the matching network is lossless, it can be easily shown that

$$\Gamma_{\mathrm{M}} = \Gamma_{\mathrm{in}}^{*} \Leftrightarrow r_{11} = 0 \text{, where } \mathbf{\Gamma}_{\mathrm{in}} = \begin{bmatrix} r_{11} & r_{12} \\ r_{12} & r_{11} \end{bmatrix}. \qquad (18)$$

However, reflection occurs into the adjacent circuit, and it can be shown that $r_{12} \neq 0$ iff $\left[\mathbf{S}_{\mathrm{RR}}\right]_{ij} \neq 0$ and $\left[\mathbf{S}_{12}\right]_{ij} \neq 0$, $\forall i \neq j$. Nevertheless, the condition $r_{11} = 0$ is sufficient for the complex correlation to be zero in the presence of a 3D uniform APS [31]. The behavior of $|r_{11}|$ and $|r_{12}|$ as described above can be observed along the center frequency in Fig. 11(e) and 11(f).

Likewise, for the MC match, since $r_{11} = r_{12} = 0$ at the center frequency, the antenna correlation is also zero for the uniform 3D APS [31]. For any other distribution, it is also possible to enforce zero correlation by appropriate design of $\mathbf{S}_{21}$ and $\mathbf{S}_{12}$ [12]. It can be seen in Figs. 11(g) and 11(h) that $|r_{11}|$ and $|r_{12}|$ are nearly, but not exactly, zero. The slight discrepancy is due to the best effort implementation of the MC match, as mentioned in Section IV.

B. *Uniform 2D APS*

A uniform 2D APS is frequently used for the evaluation of antenna correlation. It is convenient as a benchmark and facilitates simplification. For antenna elements with isotropic azimuth pattern, no mutual coupling, and similarly polarized as the arriving waves, the open circuit (or field) correlation between the two antenna elements separated by distance d is given by the Clarke's formula $J_0(kd)$ [32], where $J_0(\bullet)$ is the zero-th order Bessel function of the first kind and $k = 2\pi/\lambda$ is the wave number. However, in the presence of mutual coupling, the correlation coefficients are changed [9]. Fig. 6 shows the (absolute value of) the complex antenna correlation over 120 MHz bandwidth (centered at 5.2 GHz) and $d \in [0.01\lambda, 0.6\lambda]$ for four different matching conditions.

The first observation in Fig. 6 is that the correlation property is relatively frequency invariant over the entire bandwidth, except for the input impedance and MC match at very small separations ($d < 0.2\lambda$). It can be seen that for very small separations, the MC match has the lowest antenna correlation at the center frequency, where it approaches 0 at $d = 0.01\lambda$. However, the correlation increases rapidly away from the center frequency. On the other hand, the input impedance match maintains a correlation value of around 0.1 down to $d = 0.01\lambda$, but has a slower increase of the correlation away from the center frequency. The Z_0 match

and the self impedance match have nearly the same performance. We note also that at small antenna separations, our result for the MC match differs from that in [12]. This is largely due to the different assumptions for the thickness of the dipoles. In [12], the dipole has a diameter of 0.02λ, and it is found that uneven current distributions around the antenna's circumference become significant when the separation is in the order of the thickness of the antenna. For our dipole of diameter $\lambda/400$, this effect is negligible in the considered range $d \in [0.01\lambda, 0.6\lambda]$. as confirmed by comparisons with a cylinder approximation of the dipole using [25]. The use of different matrix factors for $\mathbf{S}_{12}$ and $\mathbf{S}_{21}$ from (6) and (7) also contributes to a small discrepancy.

A notable common feature in all cases of Fig. 6 is the improvement in correlation as compared to the open-circuit case described by the Clarke's formula, which has a slower decay in correlation as antenna separation increases from zero and larger oscillations beyond the first zero [32]. This highlights the benefit of lower antenna correlation from current induced via mutual coupling in the adjacent antenna, which introduces pattern diversity. In the case of the Z_0 match (see Fig. 6(a)), the decrease of correlation is monotonic over the considered range of antenna separations.

C. *Outdoor-to-Indoor Channels.*

The antenna correlations in the LOS scenarios (see Fig. 7) for the different matching conditions over frequency and antenna separations are higher than those of the uniform 2D APS, while those of the NLOS scenario (see Fig. 8) come in between those two scenarios, a result that is not surprising [7]. As in the case of uniform 2D APS, antenna correlations are relatively frequency invariant in both LOS and NLOS scenarios, except for small antenna separations. At small antenna separations, the input impedance match and MC match can maintain a lower correlation than the Z_0 match and self impedance match, though the frequency regions (or bandwidths) for the lower correlation narrows with smaller antenna separations. We also note that the correlation at the center frequency for extremely low separations is much higher than in the 2D-uniform case. However, the relative frequency at which the correlation coefficient changes significantly is similar compared to the 2D uniform case.

One distinction of the LOS and NLOS scenarios from the uniform 2D case is that the matching condition can make a significant impact in the correlation value at moderate antenna separations. For example, the Z_0 match gives the lowest correlation values in the uniform 2D case for $d > 0.3\lambda$, while in the measured scenarios it has a poor performance in this region.

VII. Numerical Results: Matching Efficiency

A. *Transmitter Matching*

Fig. 9 summarizes the transmit matching efficiency η_T (16) over both antenna separation and frequency for different matching conditions, assuming that the final term of (16) is zero. We note that except for the MC match of Fig. 9(d) at small antenna separations, the efficiency measure does not vary significantly over frequency. Since the impedance Z_0 does not match either the self or mutual impedance of the antennas, the Z_0 match in Fig. 9(a) does not achieve efficiency of 1 even for larger antenna separations where mutual coupling is weaker. The perfect matching achieved by the MC match allows it to retain efficiency of 1, even for very small antenna separations, at the cost of a narrowing frequency band in which this desirable performance is achieved. The (partially-matched) self impedance match in Fig. 9(b) has a performance between the two other cases, and it approaches the efficiency of the MC match at larger antenna separations (where mutual coupling is weaker). From Fig. 9(c), we see that the efficiency of the input impedance match tends to zero for very small antenna separations, even though $|r_{11}| = 0$ is maintained at the center frequency. As can be seen in Fig. 11(f), which gives $|r_{12}|$ for the input impedance match, the loss in efficiency is due to increasing transmission into the adjacent circuits when antenna separations are small, i.e. $|r_{12}| \to 1$ as $d \to 0$.

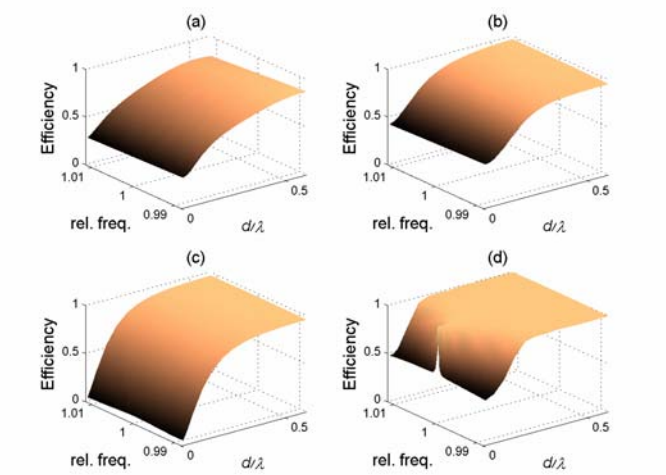

Fig. 9. Matching efficiency of transmitter at different antenna separations for different matching conditions: (a) Z_0 match, (b) Self Impedance match, (c) Input impedance match, and (d) MC match.

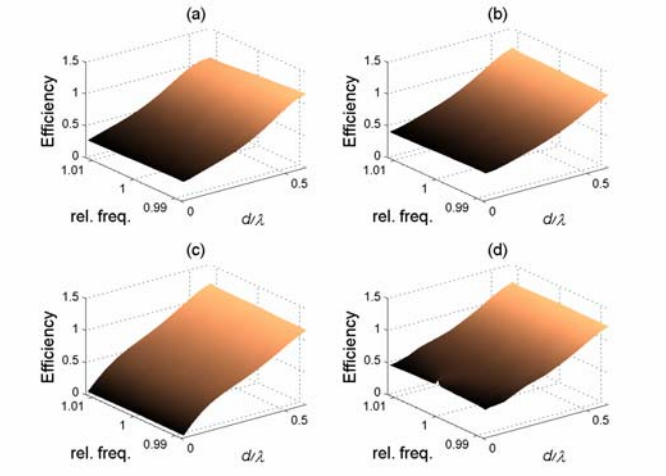

Fig. 10. Matching efficiency of receiver at different antenna separations for different matching conditions and LOS condition: (a) Z_0 match, (b) Self impedance match, (c) Input impedance match, and (d) MC match.

B. Receiver Matching with Uniform 2D APS

For the receiver, the situation is more complicated, as the matching efficiency η_R depends on the angular spectrum of the incident radiation. For a uniform 2D APS, the results are nearly identical to those of the transmit case (Fig. 9), and thus not shown graphically. The similarity arises because the received power at the antenna ports can be modeled by excitation sources (open circuit voltages), as in Fig. 5. As in the transmit case, the amount of mismatch between the antennas and the matching network determines how much power is transmitted through the network, which in the receive mode equals the received load power. For example, the MC match maximizes the received load power for the multiple antenna case at the center frequency [12].

As pointed out earlier, the main distinction of the receive mode from the transmit mode is that the open-circuit voltages sources are determined by the antenna pattern and the propagation environment. For uniform 2D APS, this open-circuit correlation has a minor effect on the efficiency, except for the MC match. For the MC match, even though the efficiency maintains a similar form to Fig. 9(d), the receive efficiency at the center frequency exceeds 1 (or $\eta_R > 1$) in the region $d < 0.4\lambda$ and rises to a maximum value of 1.1 at $d = 0.03\lambda$. This is consistent with the observation in Fig. 7 of [16], which is attributed in [16] to the power scattered by each receive antenna being recaptured by the adjacent antennas. Note, however, again the difference of our results compared to those of [16] at very small antenna separations, due to the different dipole models and matrix factorizations.

C. Receiver Matching with Outdoor-to-Indoor Channels.

Fig. 10 illustrates the receive efficiency η_R for the LOS environment of the outdoor-to-indoor measurement campaign. For the narrow angular spread of the LOS channel, the correlation between open-circuit voltages mentioned above becomes a dominant factor for the matching efficiency. In particular, we note that the high open-circuit correlation causes a degradation in the efficiency of the antenna array (with respect to the single antenna case) for antenna separation $d < 0.5\lambda$ (see Fig. 10). As the antenna separation tends to 0, the open circuit correlation tends to 1, and therefore the efficiency behavior becomes almost independent of the APS (cf. Figs 9 and 10). The only exception is the MC match close to the center frequency. There, the efficiency of close to 1 is the direct result of uniform 2D APS giving low antenna correlation in Fig. 6(d). In Fig. 10(d), it is observed that both the amplitude and width of the "efficiency peak" at the center frequency greatly diminish at very small antenna separations. As the open-circuit correlation reduces progressively with larger antenna separation, the efficiency increases beyond 1 for $d > 0.5\lambda$. It should be noted that while some phenomena can be conveniently explained in terms of single dominant factor, the received load voltage (4) (and thus power) is in general the combined effects of the open-circuit voltages, the antennas and the matching network.

The NLOS scenario falls in between the uniform 2D APS and the LOS scenario, and the efficiency plot is not included here due to space constraint. It is clear from comparing Fig. 9 and 10 that angular spread can distort to a large degree matching efficiency of the receive subsystem (remembering that the receive matching efficiency for the uniform 2D case is nearly identical to Fig. 9). In a scenario with small angular spread, such as that of the LOS scenario, the more sophisticated MC match does not have a significant benefit over the simple, individual-port self impedance match.

VIII. Numerical Results: Bandwidth

A. Efficiency Bandwidth

Fig. 11 shows the behaviors of $|r_{11}|$ and $|r_{12}|$ over frequency and antenna separation for different matching conditions. For the Z_0 match (Figs. 11(a) and 11(b)), $|r_{11}|$ and $|r_{12}|$ show only small variations as a function of frequency. Since there is no matching network, any variations arise from the frequency dependent properties of the antennas themselves. A Z_0 matched single dipole of the specified thickness has a bandwidth of around 14.3% (at a resonant frequency of 4.88 GHz) for a return loss of −6 dB (see Fig. 7.5 in [25]). On the other hand, $|r_{11}|$ and $|r_{12}|$ vary with d according to the self and mutual impedances, in the same trend as Fig. 4 in [16]. In particular, $|r_{12}|$ becomes increasingly large at closer separation, due to the strong coupling into the adjacent circuit.

The use of self impedance match clearly improves $|r_{11}|$, as compared to the Z_0 match (compare Figs. 11(a) and 11(c)). This is not surprising, as it matches the self impedance of the dual-antenna system. However, as opposed to the self impedance match for the single antenna case, where the return loss around the center frequency is like a narrow valley, and takes on a very small value at the center frequency, $|r_{11}|$ takes on moderate values at the center frequency, with troughs occurring off the center frequency. This is because $|r_{11}|$ depends on *both* the self and mutual impedances, and the mutual impedance neglected by this matching condition is significant at the given range of antenna separations. Moreover, no apparent improvement is seen in Fig. 11(d) (compared to Fig. 11(b)) for $|r_{12}|$, again because mutual impedance is not matched.

For the input impedance match, it was shown analytically in Section VI-A that at the center frequency, $|r_{11}|$ and $|r_{12}|$ are zero and non-zero, respectively. Due to explicit matching carried out for $|r_{11}|$, the desirable valley-like response is observed around the center frequency in Fig. 11(e). However, since the input impedance match does not maximize power transfer into the antenna, $|r_{12}|$ takes on the highest value at the center frequency for any antenna separation (see Fig. 11(f)). Moreover, $|r_{12}|$ tends to one as antenna separation decreases.

It can be seen in Figs. 11(g) and 11(h) that for a narrowband system, the MC match appears to present a more attractive matching solution, as it has a fairly even performance for $|r_{11}|$ *and* $|r_{12}|$. Unfortunately, it is nontrivial to obtain a well optimized solution using the procedure in [30] and the optimized point is non-robust to small perturbations in the lengths of the circuit elements used (especially for very

small antenna separations). We also note that the bandwidth becomes extremely narrow at small antenna separations. This is also exemplified in the efficiency performance in Fig. 9(d). Arguably, better bandwidth performance can be achieved by a different implementation of the MC match than that of [30]. For the single antenna case, the Bode-Fano criterion [27] defines an upper bound for achievable antenna bandwidth with any matching. To date, such results are unavailable for multiple antennas. However, since it is well known that the simple transmission line and open-circuited stub configuration is inefficient relative to the Bode-Fano bound [27], it is fair to anticipate that the bandwidth of the MC match implemented with simple combinations of these circuit elements [30] is likewise far from its fundamental limits.

In Fig. 12(a), the fractional efficiency bandwidth (based on definition (17)) is given for a −6 dB return loss. The Z_0 match has the poorest bandwidth performance, and is undefined for $d < 0.3\lambda$. This is mainly due to the finite thickness of the λ/2-dipole antenna, which results in the resonant frequency not exactly at the designed frequency of 5.2 GHz. Moreover, the efficiency bandwidth is also undefined for self impedance match and input impedance match for $d < 0.15\lambda$ and $d < 0.2\lambda$, respectively, as the mutual coupling is severe and results in poor return loss $|r_{12}|$, which dominates the efficiency behavior. It can be seen from Fig. 12(a) that the MC match is the only matching that gives a definable bandwidth when $d < 0.15\lambda$, even though there is a drastic drop in bandwidth with decreasing antenna spacing. At $d = 0.1\lambda$, the fractional bandwidth is just over 2%, which contrasts sharply with 10-20% bandwidth that can be obtained with either the self impedance match or the input impedance match for $d \geq 0.2\lambda$.

For comparison, the return losses of a single λ/2-dipole of the same thickness with the Z_0 match and self impedance match were also calculated. The fractional bandwidth using definition (17) is at a mere 4.6% for a −6 dB return loss for the single antenna with the Z_0 match. This is because without matching, the resonant frequency (4.88 GHz) is about 6% lower than the desired center frequency of 5.2 GHz due to finite antenna thickness. On the other hand, the self impedance match gives a fractional bandwidth of 17.8%, which is in good agreement to the achieved bandwidths of the self impedance match and input impedance match shown in Fig. 12(a) for $d \geq 0.2\lambda$.

As mentioned in Section V-C, the matching efficiency in the transmit and receive modes, which include those shown in Figs. 9 and 10, can give a more comprehensive description of efficiency bandwidth than definition (17). This is because they are based on actual radiated and received powers, rather than only the dominant reflectance(s) (which in this case is either $|r_{11}|$ or $|r_{12}|$). For comparison, the bandwidths found from these alternative definitions of matching efficiency bandwidth are summarized in Figs. 12(b), 12(c), 13(a) and 13(b), respectively. Note that all values of the plots in Fig. 13 are clipped to a maximum fractional bandwidth of 2.3%, since the outdoor-to-indoor channels are measured within this bandwidth and are only strictly valid in this region.

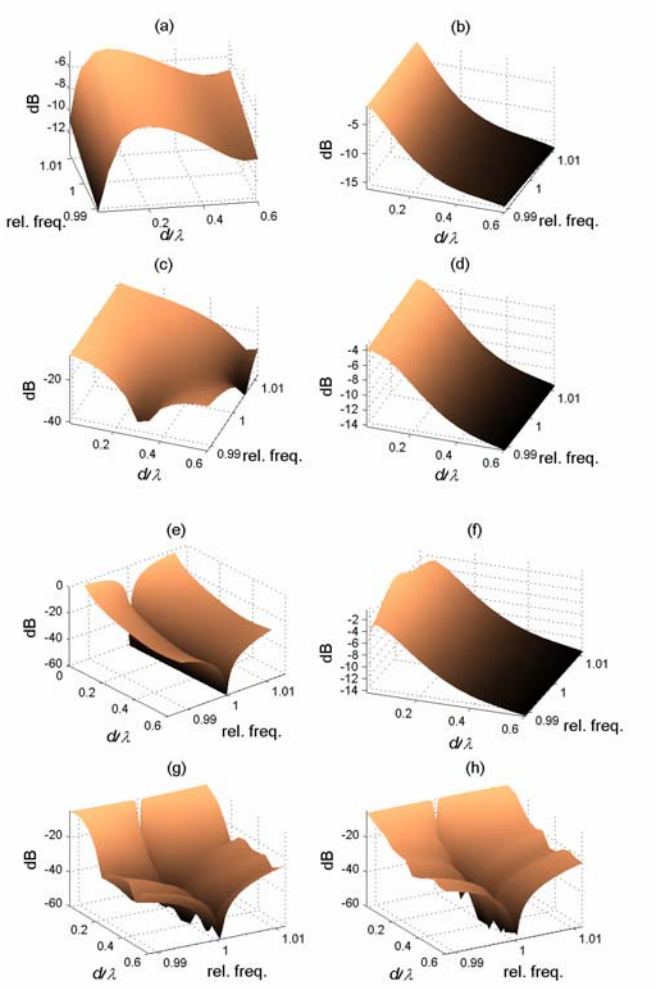

Fig. 11. $|r_{11}|$ and $|r_{12}|$ over different antenna separations and frequency points for different terminations: (a) $|r_{11}|$ and (b) $|r_{12}|$ for Z_0 match, (c) $|r_{11}|$ and (d) $|r_{12}|$ for self impedance match, (e) $|r_{11}|$ and (f) $|r_{12}|$ for input impedance match, (g) $|r_{11}|$ and (h) $|r_{12}|$ for MC match.

First, we compare between definition (17) and the transmit efficiency bandwidth. A quick comparison between Figs. 12(a) and 12(b) confirms that the less precise definition (17) tends to overestimate the efficiency bandwidth. In fact, bandwidth is defined for the Z_0 match and the self impedance match for $d \geq 0.3\lambda$ and $d \geq 0.15\lambda$, respectively in Fig. 12(a), while for Fig. 12(b) this is when $d \geq 0.35\lambda$ and $d \geq 0.2\lambda$, respectively. The bigger discrepancies in bandwidths of the Z_0 match, self impedance and input impedance match than the MC match (in absolute terms) between Figs. 12(a) and 12(b) are mainly due to $|r_{12}|$ being significant around the center frequency, as opposed to the case of MC match (compare Figs. 11(b), 11(d) and 11(f) with Fig. 11(h)).

While the bandwidths shown in Figs. 12(a) and 12(b) are suitable for evaluating efficiency performance at the transmitter, the efficiency at the receiver depends also on the prevalent propagation condition. The efficiency bandwidths in the receive mode for different matching conditions in a uniform 2D APS are summarized in Fig. 12(c). It is observed that the efficiency bandwidth demonstrates a trend similar to that of the transmit mode, due to the similarity between their

matching efficiency performances (see Sections VII-A and VII-B). One common feature in Figs. 12(a)-12(c) is that the MC match has slightly smaller bandwidths than the self impedance match and input impedance match for $d \geq 0.2\lambda$. This is primarily due to its implementation using the optimization procedure in [30], in which the objective is to obtain $r_{11} = r_{12} = 0$ at the center frequency, rather than maximum bandwidth. As an example, the valley-like behavior of $|r_{11}|$ and $|r_{12}|$ in Figs. 11(g) and 11(h) can have asymmetries which decrease the bandwidth. Therefore, larger bandwidths can be obtained through a more appropriate formulation.

On the other hand, the efficiency bandwidth of the measured LOS channel is only defined for $d \geq 0.35\lambda$ for the MC match and $d \geq 0.4\lambda$ for the other three matching conditions (see Fig. 13(a)). As in the case of matching efficiency, the efficiency bandwidths of the NLOS scenario fall between those of the LOS and the uniform 2D cases. As can be seen in Fig. 13(b), while bandwidth is consistently defined for the MC match, bandwidth is only defined for both the self impedance match and the input impedance match for $d \geq 0.25\lambda$, and the Z_0 match for $d \geq 0.4\lambda$.

From the above discussion, we conclude that while efficiency bandwidths can vary considerably among the different definitions, the MC match gives the most consistent bandwidth performance for $d \in [0.01\lambda, 0.6\lambda]$. Nevertheless, the propagation environment can in some cases overwrite its benefits for the receive mode. Therefore, it is important to consider the effect of the propagation channel in the design of receiver for multiple antenna systems.

B. *Correlation Bandwidth*

While efficiency bandwidth can be defined in different ways, as shown above, correlation bandwidth is uniquely defined (for a given threshold value). Fig. 12(d) illustrates the correlation bandwidth for the case of uniform 2D APS and a threshold of $|\rho| = 0.71$. As can be seen, all matching conditions give correlation bandwidth of over 10% for $d \geq 0.15\lambda$. The correlation bandwidths are clipped at a maximum value of 30%, since it is clear from Fig. 12(c) that the efficiency bandwidth is the limiting factor to the performance of the receive antennas.

The correlation bandwidth for the LOS scenario in Fig. 13(c) reveals that the bandwidth is defined for both input impedance match and MC match when $d \leq 0.35\lambda$, and for self impedance match when $d \in [0.25\lambda, 0.35\lambda]$. This is in contrast to the efficiency bandwidth which is only defined at a range of larger antenna separations. This implies that for the LOS scenario, the design of the receive subsystem fails to simultaneously satisfy the specified requirements for correlation *and* efficiency.

As in the uniform 2D APS case, when compared to the receive efficiency bandwidth in Fig. 13(b), the correlation bandwidth of Fig. 13(d) is clearly not the limiting factor in the compact antenna performance in the considered 2.3% bandwidth in the NLOS scenario.

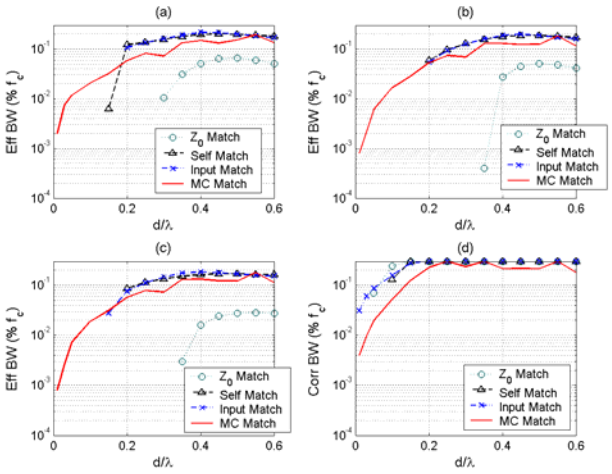

Fig. 12. Efficiency bandwidths for (a) definition (17), (b) transmit mode of Fig. 9, (c) receive mode; and (d) correlation bandwidth in receive mode of Fig. 6, over different antenna separations for different matching conditions.

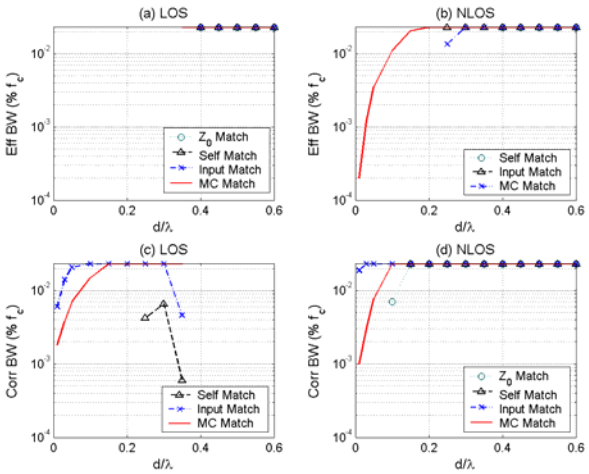

Fig. 13. Efficiency bandwidths in (a) LOS and (b) NLOS, and correlation bandwidths in (c) LOS and (d) NLOS, over different antenna separations for different matching conditions.

In practice, explicit results of efficiency and correlation bandwidths, such as those given in Figs. 12 and 13 not only provide useful insights into the influence of matching condition and propagation environment, it readily yield information as to whether the antenna system can be used for a specific wireless communication system. For example, a WCDMA mobile terminal requires an uplink frequency band of 1.92 GHz to 1.98 GHz and a downlink band of 2.11 GHz to 2.17 GHz. This translates to a fractional bandwidth of 12.2% and a center frequency of 2.045 GHz. Assuming that the uniform APS is the typical operating environment, the transmit and receive efficiency bandwidths (Figs. 12(b) and 12(c)), as well as the correlation bandwidth (Fig. 12(d)), satisfy this requirement with either the self or input impedance match at a minimum $d = 0.25\lambda$ (or 3.67 cm). On the other hand, if an IEEE802.11b-enabled PDA operates in the frequency band from 2.4 GHz to 2.5 GHz, representing a fractional bandwidth of 4.1%, then the more sophisticated MC

match can be used to bring down the minimum required separation to $d = 0.15\lambda$ (or 1.84 cm).

IX. Conclusion

In this paper, we showed that matching plays a vital role in the wideband performance of compact multiple antenna systems. Moreover, different matching networks affect the bandwidths of antenna correlation and matching efficiency in different ways. For example, while the input impedance match can give a 10% correlation bandwidth at a small antenna separation of 0.1λ, the efficiency bandwidth is undefined for a −6 dB return loss. On the other hand, MC match can simultaneously fulfill the requirements of low correlation and good matching efficiency at the center frequency, but the bandwidths for small antenna separations are significantly smaller than the efficiency bandwidth in the optimally matched single antenna case (e.g., less than 2% at d =0.1λ vs. 17.8%). At very small antenna separations, useful (or "sufficiently large") bandwidth cannot be obtained with the implementations used in our study. This provides some important practical limitations, which complement the theoretical limitations of densely packing antennas into small volumes as pointed out in [33]-[35]. We also note that practical small antennas (usually a small fraction of a wavelength) are inherently lossy and such losses lead to a wider bandwidth, an effect not examined in this paper. We also showed that the propagation environment has a significant influence on the performance of multiple antenna systems in the receive mode.

Even though our results indicate that LOS channels give poorer correlation and efficiency bandwidth performances than the NLOS channels or uniform 2D APS, due to lower scattering richness or smaller angular spread, recent indoor measurement campaigns [36], [37] have shown that LOS positions tend to have much higher SNRs than NLOS positions. The difference in received power can adequately compensate for the poorer correlation and efficiency to give better performance than the NLOS cases. Indeed, for a constant transmit power of 33 dBm in our case, the SNRs of the LOS and NLOS positions were 16.7 dB and 4.3 dB, respectively [23].

On a final note, matching network cannot replace good antenna design. In practice, antennas should be designed to give desirable characteristics as much as possible, while matching network can play a complementary role for further performance improvements.

Appendix

A. Derivation of Input Impedance Match

Equation (10) can be written as

$$Z_{\mathrm{M}}^{*} = Z_{11} - Z_{12}^{2} \big/ \left(Z_{22} + Z_{\mathrm{M}}\right). \tag{19}$$

Multiplying both sides by $Z_{22} + Z_{\mathrm{L}}$ and rearranging

$$\left(Z_{\mathrm{M}}^{*} + Z_{11}\right)\left(Z_{22} + Z_{\mathrm{M}}\right) + Z_{12}Z_{21} = 0. \tag{20}$$

For the case of symmetrical dipoles $Z_{11} = Z_{22}$. We further let $Z_{\mathrm{M}} = R_{\mathrm{M}} + jX_{\mathrm{M}}$, $Z_{11} = R_{11} + jX_{11}$, and $Z_{12} = R_{12} + jX_{12}$ in (20), and after some straightforward simplifications,

$$X_{\mathrm{M}} = \frac{R_{12}X_{12}}{R_{11}} - X_{11} \text{ and}$$

$$R_{\mathrm{M}} = \pm\left(R_{11}^{2} - R_{12}^{2} + X_{12}^{2} - \frac{R_{12}^{2}X_{12}^{2}}{R_{11}^{2}} \right)^{1/2}. \tag{21}$$

The term within the square-root must be real by definition. Indeed,

$$\left(R_{11}^{2} - R_{12}^{2}\right) + X_{12}^{2} - \frac{R_{12}^{2}X_{12}^{2}}{R_{11}^{2}} = \left(R_{11}^{2} - R_{12}^{2}\right)\left(1 + \frac{X_{12}^{2}}{R_{11}^{2}}\right), \tag{22}$$

which requires $(R_{11}^{2} - R_{12}^{2}) > 0$. It is well-known that $\mathrm{Re}\{Z_{11}\} > \mathrm{Re}\{Z_{12}\} \Leftrightarrow R_{11} > R_{12}$.

Next, the negative solution of R_{L} is discarded, since the antenna only contains passive elements. Finally, the unique solution of (19) is obtained as

$$Z_{\mathrm{M}}^{\mathrm{opt}} = \sqrt{R_{11}^{2} - R_{12}^{2} + X_{12}^{2} - \frac{R_{12}^{2}X_{12}^{2}}{R_{11}^{2}}} + j\left(\frac{R_{12}X_{12}}{R_{11}} - X_{11} \right). \tag{23}$$

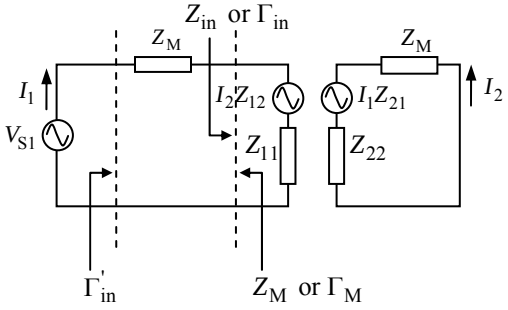

Fig. 14. Equivalent circuit for a two-dipole configuration.

Acknowledgment

We thank Shurjeel Wyne and Gunnar Eriksson for supplying the processed data from the outdoor-to-indoor measurement campaign [23]. Helpful discussions with Mats Gustafsson and Serene S. M. Ow are gratefully acknowledged.

References

[1] J. Winters, "On the Capacity of Radio Communication Systems with Diversity in a Rayleigh Fading Environment," *IEEE J. Select. Areas Commun.*, vol. SAC-5, pp.871-878, Jun. 1987.

[2] I. E. Telatar, "Capacity of multi-antenna Gaussian channels," *European Trans. Telecommun.*, vol. 10, pp. 585-595, 1999.

[3] G. J. Foschini and M. J. Gans, "On limits of wireless communications in a fading environment when using multiple antennas," *Wireless Personal Communications* (Kluwer Academic Publishers), vol. 6, pp. 311–335, Mar. 1998.

[4] D. Gesbert, M. Shafi, D. S. Shiu, P. J. Smith, and A. Naguib, "From theory to practice: an overview of MIMO space-time coded wireless systems," *IEEE J. Select. Areas Commun.*, vol. 21, no. 3, pp. 281-302, Apr. 2003.

[5] S. N. Diggavi, N. Al-Dhahir, A. Stamoulis, and A. R. Calderbank, "Great expectations: The value of spatial diversity in wireless networks," *Proc. IEEE*, vol. 92, pp. 219-270, Feb. 2004.
[6] A. F. Molisch, *Wireless Communications*, John Wiley and Sons, 2005, ch. 20.
[7] D. S. Shiu, G. J. Foschini, M. J. Gan, J. M. Kahn, "Fading correlation and its effect on the capacity of multielement antenna systems," *IEEE Trans. Commun.*, vol. 48, pp. 502-513, Mar. 2000.
[8] A. F. Molisch and F. Tufvesson, "MIMO capacity and measurements", in *Smart Antennas - State of the Art*, T. Kaiser, Ed. Hindawi, 2005, ch. 24, pp. 467-490.
[9] R. G. Vaughan and N. L. Scott, "Closely spaced monopoles for mobile communications," *Radio Science*, vol. 28, pp. 1259-1266, Nov-Dec 1993.
[10] R. Vaughan and J. B. Andersen, *Channels, Propagation and Antennas for Mobile Communications*, The IEE, 2003.
[11] P. S. Kildal and K. Rosengren, "Electromagnetic analysis of effective and apparent diversity gain of two parallel dipoles," *IEEE Antennas and Wireless Propagat. Lett.* , vol. 2, no. 1, pp. 9-13, 2003.
[12] J. W. Wallace and M. A. Jensen, "Termination-dependent diversity performance of coupled antennas: Network theory analysis," *IEEE Trans. Antennas Propagat*., vol. 52, pp. 98-105, Jan. 2004.
[13] T. Svantesson and A. Ranheim, "Mutual coupling effects on the capacity of multielement antenna systems," *Proc. IEEE ICASSP*, vol. 4, pp. 2485-2488, Salt Lake City, Utah, May 7-11, 2001.
[14] M. K. Ozdemir, E. Arvas, and H. Arslan, "Dynamics of spatial correlation and implications on MIMO systems," *IEEE Commun. Mag.*, vol. 42, pp. S14-S19, Jun. 2003.
[15] B. Clerckx, D. Vanhoenacker-Janvier, C. Oestges, and L. Vanderdorpe, "Mutual coupling effects on the channel capacity and the space-time processing of MIMO communication systems," in *Proc. IEEE ICC*, vol. 4, pp. 2638-2642, Anchorage, Alaska, 11-15 May 2003.
[16] J. W. Wallace and M. A. Jensen, "Mutual coupling in MIMO wireless systems: a rigorous network theory analysis," *IEEE Trans. Wireless Commun*., vol. 3, pp. 1317-1325, Jul. 2004.
[17] V. Jungnickel, V. Pohl, and C. von Helmolt, "Capacity of MIMO systems with closely spaced antennas," *IEEE Commun. Lett.*, vol. 7, no. 8, pp. 361-363, Aug. 2003.
[18] R. Janaswamy, "Effect of element mutual coupling on the capacity of fixed length linear arrays," *IEEE Antennas and Wireless Propagat. Lett.*, vol. 1, no. 8, pp. 157-160, 2002.
[19] P. N. Fletcher, M. Dean, and A. R. Nix, "Mutual coupling in multi-element array antennas and its influence on MIMO channel capacity," *Electron. Lett.*, vol. 39, no. 4, pp. 342-344, 20 Feb. 2003.
[20] C. Waldschmidt, S. Schulteis, and W. Wiesbeck, "Complete RF system model for analysis of compact MIMO arrays," *IEEE Trans Vehic. Technol*., vol. 53, no. 3, pp. 579-586, May 2004.
[21] S. M. S. Ow, "Impact of mutual coupling on compact MIMO systems," M.Sc. Thesis, Dept. Electroscience, Lund University, Lund, Sweden, Mar. 2005. Available: http://www.es.lth.se/teorel/Publications/TEAT-5000-series/TEAT-5074.pdf.
[22] K. Rosengren, J. Carlsson, and P. S. Kildal, "Maximizing the effective diversity gain of two parallel dipoles by optimizing the source impedances," *Microwave Opt. Tech. Lett.*, vol. 48, no. 3, pp. 532-535, Mar. 2006.
[23] S. Wyne, P. Almers, G. Eriksson, J. Kåredal, F. Tufvesson, and A. F. Molisch, "Outdoor to indoor office MIMO measurements at 5.2 GHz," in *Proc. IEEE 60th VTC Fall*, vol. 1, pp. 101-105, Los Angeles, CA, 26-29 Sep. 2004.
[24] H. Steyskal and J. S. Herd, "Mutual coupling compensation in small array antennas," *IEEE Trans. Antennas Propagat.*, vol. 38, pp. 1971-1975, Dec. 1990.
[25] S. N. Makarov, *Antenna and EM Modeling with MATLAB®*, Wiley-Interscience, 2002.
[26] A. F. Molisch, M. Steinbauer, M. Toeltsch, E. Bonek, and R. S. Thoma, "Capacity of MIMO systems based on measured wireless channels," *IEEE J. Select. Areas Commun.*, vol.20, no. 3, pp. 561-569, Apr. 2002.
[27] D. M. Pozar, *Microwave Engineering*, New York: Wiley, 1998, ch. 4.
[28] J. B. Andersen and B. K. Lau, "On closely coupled dipoles in a random field", *IEEE Antennas and Wireless Propagat. Lett*., vol. 5, no. 1, pp. 73-75, 2006.
[29] H. J. Chaloupka and X. Wang, "On the properties of small arrays with closely spaced antenna elements," in *Proc. IEEE Antennas and Propagation Society International Symposium*, vol. 3, pp. 2699-2702, Monterey, CA, 20-25 Jun. 2004.
[30] S. Dossche, S. Blanch, and J. Romeu, "Optimum antenna matching to minimise signal correlation on a two-port antenna diversity system," *Electronic Lett*., vol. 40, no. 19, pp. 1164-1165, 16 Sep. 2004.
[31] S. Stein, "On cross coupling in multiple-beam antennas," *IEEE Trans. Antennas Propagat*., vol. AP-10, no. 5, pp. 548-557, Sep. 1962.
[32] R. H. Clarke, "A statistical theory of mobile-radio reception," *Bell Syst. Tech. J.*, vol. 47, no. 6, pp. 957-1000, 1968.
[33] L. Hanlen and M. Fu, "Wireless communication systems with spatial diversity: a volumetric model," *IEEE Trans. Wireless Commun*., vol. 5, no. 1, pp. 133-142, Jan. 2006.
[34] L. W. Hanlen and M. Fu, "Capacity of MIMO channels: A volumetric approach," in Proc. *IEEE ICC*, vol. 5, pp. 3001-3005, Anchorage, Alaska, 11-15 May 2003.
[35] A. S. Y. Poon, R. W. Brodersen, and D. N. C Tse, "Degrees of freedom in multiple-antenna channels: A signal space approach," *IEEE Trans. Inform. Theory*, vol. 51, no. 2, pp. 523-536, Feb. 2005.
[36] D. P. McNamara, M. A. Beach, P. N. Fletcher, and P. Karlsson, "Capacity variation of indoor multiple-input multiple-output channels," *Electron. Lett.*, vol. 36, pp. 2037–2038, 23 Nov. 2000.
[37] M. Herdin, H. Ozcelik, H. Hofstetter, and E. Bonek, "Variation of measured indoor MIMO capacity with receive direction and position at 5.2 GHz," *Electronics Lett.*, vol. 38, pp. 1283–1285, 10 Oct. 2002.

B. K. Lau (S'00–M'03) received the BE(Hons) and Ph.D degrees in electrical engineering from the University of Western Australia and Curtin University of Technology, Australia, in 1998 and 2003, respectively.

During 2000-2001, he took a year off from his Ph.D studies to work as a Research Engineer at Ericsson Research in Kista, Sweden. From 2003 to 2004, he was a Guest Research Fellow at the Department of Signal Processing, Blekinge Institute of Technology, Sweden. He now holds a joint Research Fellow appointment at the Radio Systems group and the Electromagnetic Theory group in the Department of Electroscience, Lund University, Sweden, and during 2005, he was a Visiting Researcher at the Laboratory for Information and Decision Systems, Massachusetts Institute of Technology, USA. Dr Lau's research interests include array signal processing, wireless communication systems, and antennas and propagation.

J. B. Andersen (M'68–SM'78–F'92–LF'02) received the M.Sc. and Dr.Techn. degrees from the Technical University of Denmark (DTU), Lyngby, Denmark, in 1961 and 1971, respectively. In 2003 he was awarded an honorary degree from Lund University, Sweden. From 1961 to 1973, he was with the Electromagnetics Institute, DTU and since 1973, he has been with Aalborg University, Aalborg, Denmark, where he is now a Professor Emeritus.

He has been a Visiting Professor in Tucson, Arizona, Christchurch, New Zealand, Vienna, Austria, and Lund, Sweden. From 1993-2003, he was Head of the Center for Personkommunikation (CPK), dealing with modern wireless communications. He has published widely on antennas, radio wave propagation, and communications, and has also worked on biological effects of electromagnetic systems. He was on the management committee for COST 231 and 259, a collaborative European program on mobile communications.

Professor Andersen is a Life Fellow of IEEE and a former Vice President of the International Union of Radio Science (URSI) from which he was awarded the John Howard Dellinger Gold Medal in 2005.

G. Kristensson received his B.S. degree in mathematics and physics in 1973, and the Ph.D. degree in theoretical physics in 1979, both from the University of Göteborg, Sweden. In 1983 he was appointed Docent in theoretical physics at the University of Göteborg.

During 1977-1984 he held a research position sponsored by the National Swedish Board for Technical Development (STU) and he was Lecturer at the Institute of Theoretical Physics, Göteborg from 1980--1984. In 1984--1986 he was a Visiting Scientist at the Applied Mathematical Sciences group, Ames Laboratory, Iowa State University. He held a Docent position at the Department of Electromagnetic Theory, Royal Institute of Technology, Stockholm during 1986--1989, and in 1989 he was appointed the Chair of Electromagnetic Theory at Lund Institute of Technology, Sweden.

In 1992 and 1997 he was a Visiting Erskine Fellow at the Department of Mathematics, University of Canterbury, Christchurch, New Zealand. Currently, Gerhard Kristensson is a member of the Advisory Board of Inverse Problems, the Board of Editors of Wave Motion, and the Editorial and Review Board of Journal of Electromagnetic Waves and Applications and Progress in Electromagnetic Research. He is a Fellow of the Institute of Physics, and the Official Member of URSI, Commission B for Sweden.

Kristensson's major research interests are focused on wave propagation in inhomogeneous media, especially inverse scattering problems. During recent years the propagation of transient electromagnetic waves in complex media, such as dispersive anisotropic and bi-isotropic media, has been stressed. High frequency scattering methods, asymptotic expansions, optical fibers, antenna problems, and mixture formulas are also of interest, as well as radome design problems and homogenization of complex materials.

Andreas F. Molisch (S'89–M'95–SM'00–F'05) received the Dipl. Ing., Dr. techn., and habilitation degrees from the Technical University Vienna (TU Vienna), Vienna, Austria, in 1990, 1994, and 1999, respectively. From 1991 to 2000, he was with the TU Vienna, where he became an associate professor in 1999. From 2000 to 2002, he was with the Wireless Systems Research Department, AT&T Laboratories Research, Middletown, NJ. Since then, he has been a Senior Principal Member of Technical Staff with Mitsubishi Electric Research Labs, Cambridge, MA. He is also Professor and Chairholder for radio systems at Lund University, Lund, Sweden. His current research interests are MIMO systems, measurement and modeling of mobile radio channels, and UWB. He has authored, co-authored, or edited four books (among them the textbook "Wireless Communications", Wiley-IEEE press 2005), eleven book chapters, some 90 journal papers, and numerous conference contributions.

Dr. Molisch is an editor of the IEEE TRANSACTIONS ON WIRELESS COMMUNICATIONS, co-editor of a recent special issue on MIMO and smart antennas in the *Journal of Wireless Communications and Mobile Computing*, and a recent special issue of IEEE J. SELECTED AREAS OF COMMUN. on UWB. He has participated in the European research initiatives "COST 231," "COST259," and "COST273," where he was chairman of the MIMO channel working group. He is also chairman of Commission C (signals and systems) of the International Union of Radio Science (URSI), chairman of the IEEE 802.15.4a channel modeling subgroup, and the recipient of several awards.